

pH-Regulated Structural Evolution Enables Excitation-Dependent Tunable and Quasi-White-Light Emission in Tetrazole-Based d¹⁰ Coordination Polymers

Yanqing Guo^{a†}, Haitao Li^{b†}, Lu Liu^{a*}, and Rong Li^{b*}

^aNorth University of China, Taiyuan 030051, P. R. China

^bSchool of Materials Science & Engineering, Hubei University, Wuhan 430062, P. R. China

Table S1. XRD Crystallographic Data for 1-3

Compound	1	2	3
CCDC	1975825	1504873	1504881
Formula	C ₂₁ H ₁₄ CdN ₆ O ₅	C ₂₈ H ₂₂ CdN ₁₀ O ₁₀	C ₃₀ H ₂₀ N ₁₀ O ₉ Zn
Formula mass	542.78	770.96	729.93
Crystal system	Monoclinic	Triclinic	Triclinic
Space group	<i>C2/c</i>	<i>P-1</i>	<i>P-1</i>
<i>a</i> /Å	31.1727(10)	6.536(3)	10.142(2)
<i>b</i> /Å	6.8735(3)	8.817(4)	11.581(3)
<i>c</i> /Å	19.5674(7)	13.687(7)	13.244(3)
α /°	104.442(3)	93.640(6)	84.565(15)
β /°	98.575(4)	97.775(4)	76.115(11)
γ /°	104.442(3)	98.916(8)	77.104(15)
<i>V</i> /Å ³	4060.14(27)	769.18(63)	1470.63(59)
<i>Z</i>	8	1	2
ρ_{calc} g/cm ³	1.776	1.664	1.648
μ /mm ⁻¹	1.125	0.785	0.912
<i>F</i> (000)	2160	388	1789
Reflections collected	17746	6856	13278
<i>wR</i> ₂ ^b (all data)	0.053	0.070	0.179
<i>R</i> ₁ ^a [<i>I</i> > 2 <i>s</i> (<i>I</i>)]	0.020	0.028	0.034
<i>R</i> _{int}	0.0228	0.0286	0.0737

^a*R*₁ = $\sum ||F_o| - |F_c|| / \sum |F_o|$. ^b*wR*₂ = $[\sum w(F_o^2 - F_c^2)^2] / [\sum w(F_o^2)^2]^{1/2}$.

Table S2. Selected lengths (Å) and angles (°) for the as-synthesized crystals of **1**.

Cd1–O13	2.3656(11)	Cd1–N12	2.4168(13)
Cd1–N13#1	2.3683(12)	Cd1–O1W	2.4295(13)
Cd1–N16#2	2.4006(13)	Cd1–O14	2.5605(11)
Cd1–N11	2.4023(12)	N12–Cd1–O1W	84.03(5)
O13–Cd1–N13#1	104.48(4)	O13–Cd1–N16#2	84.30(4)
N13#1–Cd1–N16#2	163.01(4)	O13–Cd1–N11	78.69(4)
N13#1–Cd1–N11	93.48(4)	N16#2–Cd1–N11	102.59(4)
O13–Cd1–N12	146.86(4)	N13#1–Cd1–N12	86.60(5)
O13–Cd1–O14	52.60(3)	N16#2–Cd1–N12	93.84(4)
N13#1–Cd1–O14	92.41(5)	N11–Cd1–N12	69.41(5)
N16#2–Cd1–O14	81.33(4)	O13–Cd1–O1W	127.93(4)
N11–Cd1–O14	130.79(4)	N13#1–Cd1–O1W	82.15(4)
N12–Cd1–O14	159.77(4)	N16#2–Cd1–O1W	81.02(4)
N11–Cd1–O1W	153.32(5)	O1W–Cd1–O14	75.83(4)

Symmetry codes for 1: #1 $-x + 1/2, -y + 3/2, -z + 1$; #2 $-x + 1/2, -y + 1/2, -z + 1$.

Table S3. Selected lengths (Å) and angles (°) for the as-synthesized crystals of **2**.

Cd1–N22#1	2.3024(19)	Cd1–O1W	2.3238(17)
Cd1–N22	2.3025(19)	Cd1–N11	2.3994(19)
Cd1–O1W#1	2.3238(18)	Cd1–N11#1	2.3994(19)
N22#1–Cd1–N11#1	93.40 (7)	N22#1–Cd1–N11	86.60 (7)
N22–Cd1–N11#1	86.60 (7)	N22–Cd1–N11	93.40 (7)
O1W#1–Cd1–N11#1	89.72 (7)	O1W#1–Cd1–N11	90.28 (7)
O1W–Cd1–N11#1	90.28 (7)	O1W—Cd1—N11	89.72 (7)
N11–Cd1–N11#1	180.0	N22#1–Cd1–N22	180.0
N22#1–Cd1–O1W	90.59 (7)	N22#1–Cd1–O1W#1	89.41 (7)
N22–Cd1–O1W	89.41 (7)	N22–Cd1–O1W#1	90.59 (7)
O1W#1–Cd1–O1W	180.00 (8)		

Symmetry codes for 2: #1 $-x, -y + 1, -z + 1$; #2 $-x + 1, -y, -z + 1$.

Table S4. Selected lengths (Å) and angles (°) for the as-synthesized crystals of **3**.

Zn1–N43	2.000(3)	Zn1–O1W	2.122(3)
Zn1–N32	2.027(3)	Zn1–N11	2.179(3)
Zn1–N21	2.071(3)		
N32–Zn1–N11	90.05(13)	N21–Zn1–O1W	89.70(13)
N21–Zn1–N11	78.18(15)	N43–Zn1–N11	94.63(13)
O1W–Zn1–N11	166.75(14)	N43–Zn1–N32	112.27(13)
N43–Zn1–O1W	95.67(11)	N43–Zn1–N21	116.96(12)
N32–Zn1–O1W	93.74(12)	N32–Zn1–N21	130.02(12)

Symmetry codes for 3: #1 $-x + 1/2, -y + 3/2, -z + 1$, #2 $-x + 1/2, -y + 1/2, -z + 1$.

Table S5. Summary of SHAPE analysis for compound **1**.

Metal	label	shape	symmetry	Distortion(τ)
	HP-7	Heptagon	D_{7h}	31.886
	HPY-7	Hexagonal pyramid	C_{6v}	20.086
	PBPY-7	Pentagonal bipyramid	D_{5h}	1.916
Cd1	COC-7	Capped octahedron	C_{3v}	5.877
	CTPR-7	Capped trigonal prism	C_{2v}	4.147
	JPBPY-7	Johnson pentagonal bipyramid J13	D_{5h}	5.055
	JETPY-7	Johnson elongated triangular pyramid J7	C_{3v}	19.941

Table S6. Summary of SHAPE analysis for compound **2**.

Metal	label	shape	symmetry	Distortion(τ)
	OP-8	Octagon	D _{8h}	28.687
	HPY-8	Heptagonal pyramid	C _{7v}	25.853
	HBPY-8	Hexagonal bipyramid	D_{6h}	7.894
	CU-8	Cube	O _h	14.430
Cd	SAPR-8	Square antiprism	D _{4d}	22.786
	TDD-8	Triangular dodecahedron	D _{2d}	20.7773
	JGBF-8	Johnson gyrobifastigium J26	D _{2d}	12.965
	JETBPY-8	Johnson elongated triangular bipyramid J14	D _{3h}	22.594

Table S7. Summary of SHAPE analysis for compound **3**.

Metal	label	shape	symmetry	Distortion(τ)
	PP-5	Pentagon	D _{5h}	32.286
	vOC-5	Vacant octahedron	C _{4v}	4.312
Zn1	TBPY-5	Trigonal bipyramid	D_{3h}	1.029
	SPY-5	Spherical square pyramid	C _{4v}	2.739
	JTBPY-6	Johnson trigonal bipyramid J12	D _{3h}	3.058

Table S8. Quantitative comparison of the principal π - π interactions in compounds **1–3**, derived from the PLATON analysis.

Cg(I)-Cg(J)	Cg-Cg (Å)	Alpha (°)	CgI_Perp (Å)	Slippage (Å)
Compound 1				
Cg(R3)-Cg(R3)	3.563	0.00	3.330	1.267
Cg(R1)-Cg(R5)	3.724	13.25	3.327	2.000
Cg(R3)-Cg(R4)	3.808	0.54	3.333	1.831
Compound 2				
Cg(R2)-Cg(R2)	4.215	0.00	3.947	1.478
Cg(R3)-Cg(R3)	3.795	0.00	3.385	1.715
Compound 3				
Cg(R4)-Cg(R4)	3.596	0.00	3.343	1.325
Cg(R1)-Cg(R3)	3.634	9.07	3.535	0.567
Cg(R2)-Cg(R4)	3.666	1.05	3.370	1.427
Cg(R6)-Cg(R6)	3.693	0.00	3.567	0.957
Cg(R6)-Cg(R7)	3.856	2.78	3.545	1.434

Notes: Cg(I)/Cg(J) denote the centroids of the interacting rings. Alpha is the dihedral angle between the ring planes. Cg-Cg is the centroid-to-centroid distance. CgI_Perp is the perpendicular distance from Cg(I) to the plane of ring J. Slippage is the distance between Cg(I) and Perpendicular Projection of Cg(J) on Ring I (Ang).

Ring labels used here: **Compound 1:** R1 benzene, R3 pyridyl, R4 benzene, R5 pyridyl; **Compound 2:** R2 benzene, R3 pyridyl; **Compound 3:** R1 tetrazole, R2/R4/R6 benzene, R3 tetrazole, R7 pyridyl.

Table S9. The main hydrogen bonds for compound **1-3**

Compound 1					
Type	D–H···A	D–H (Å)	H···A (Å)	D···A (Å)	<(DHA) (°)
	O11–H1···O14	0.81(2)	1.74(2)	2.5473(18)	177(2)
	O1W–H1WA···O12	0.84(2)	2.12(2)	2.9256(18)	161(2)
Intra	O1W–H1WB···N15	0.842(12)	2.211(15)	2.8728(18)	136(2)
Intra	C11–H11A···O13	0.93	2.32	2.9711(19)	126
Intra	C22–H22A···O1W	0.93	2.58	3.224(2)	127
Compound 2					
Type	D–H···A	D–H (Å)	H···A (Å)	D···A (Å)	<(DHA) (°)
	O1W–H1WA···N23	0.837(16)	2.14(2)	2.914(3)	153(2)
	O1W–H1WB···O24	0.834(16)	1.889(16)	2.717(3)	172(3)
	O23–H27A···N24	0.74(4)	1.95(4)	2.653(3)	158(4)
	O22–H28A···O21	1.05(9)	1.54(9)	2.586(3)	174(9)
Intra	C22–H22A···O22	0.93	2.43	2.740(3)	100
Intra	C22–H22A···N21	0.93	2.52	2.847(3)	101
	C24–H24A···O23	0.93	2.40	3.283(3)	160

Compound 3					
Type	D–H···A	D–H (Å)	H···A (Å)	D···A (Å)	<(DHA) (°)
O3W–3WA...O1W		0.846(17)	2.556(17)	3.129(7)	125.9(15)
O3W–H3WB...O24		0.849(13)	2.28(3)	2.803(6)	120(2)
O3W–H3WB...N12		0.849(13)	2.124(17)	2.873(6)	147(3)
O2W–H2WA...O4W		0.85(3)	2.275(18)	2.853(9)	126(3)
O2W–H2WB...O4W		0.848(18)	2.47(3)	3.014(9)	122(2)
O1W–H1WB...O3W		0.850(17)	2.36(2)	3.129(7)	152(2)
O4W–H4WA...O24		0.85(3)	1.99(3)	2.827(8)	168(4)
O4W–H4WB...O5W		0.85(2)	2.52(3)	2.939(11)	111(3)
O6W–H6WA...O5W		0.849(18)	2.04(2)	2.829(13)	155(3)
O5W–H5WA...O23		0.849(19)	1.962(19)	2.757(9)	156(2)
C11–H11A...N23		0.93	2.46	3.381(7)	172
C34–H34A...O3W		0.93	2.59	3.127(7)	117

Table S10. The corresponding CIE coordinates (x, y), CRI and CCT values for **1** under different excitation wavelengths.

λ_{ex} / nm	CIE (x, y)	CRI	CCT
300	(0.219 0.232)	86	3349

320	(0.232 0.212)	93	5863
340	(0.236 0.222)	94	3841
360	(0.247 0.246)	92	1649
380	(0.263 0.313)	81	2784
400	(0.284 0.366)	75	3944

Table S11. Fluorescence decay parameters of compound 1-3.

Compound	λ_{em} / nm	τ_1 (ns)	A_1	τ_2 (ns)	A_2	τ (ns)
1	500	1.39	0.52	7.24	0.48	4.2
2	485	6.82	0.51	15.89	0.49	11.3
3	500	3.45	0.42	10.20	0.58	7.37

The lifetime data were processed according to the literature method.¹ Decay in the fluorescence intensity (I) with time (τ) was fitted by a double-exponential function: $I = A_1 \exp(-t / \tau_1) + A_2 \exp(-t / \tau_2)$ (1), where τ_1 and τ_2 are the lifetimes of shorter- and longer-lived species, respectively, and A_1 and A_2 are their respective amplitudes. The weighted mean lifetime ($\langle \tau \rangle$) was calculated according to Equation (2): $\langle \tau \rangle = (A_1 \tau_1 + A_2 \tau_2) / (A_1 + A_2)$.

(1). Qin, A.; Jim, C. K.; Tang, Y.; Lam, J. W.; Liu, J.; Mahtab, F.; Gao, P.; Tang, B. Z. *J. Phys. Chem. B*, 2008, **112**, 9281–9288.

Table S12. Solid-state photoluminescence quantum yields (PLQYs) of compounds 1–3 measured under 400 nm excitation.

Compound	Excitation wavelength / nm	PLQY/%
1	400	5.53
2	400	6.65
3	400	5.21

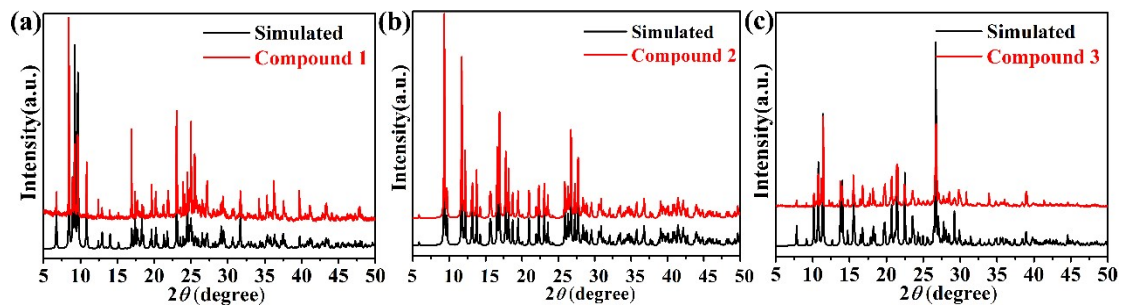


Figure S1. Comparison of experimental PXRD patterns for compound **1** (a), compound **2** (b) and compound **3** (c) to their simulated ones from single-crystal X-ray data.

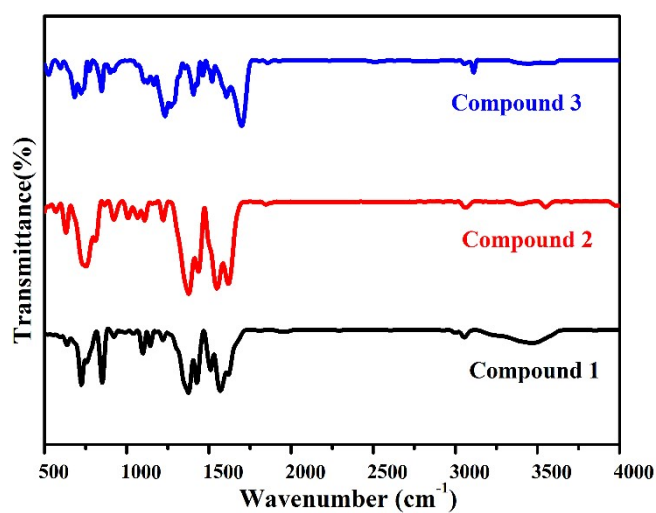


Figure S2. FT-IR curves for compound **1-3**

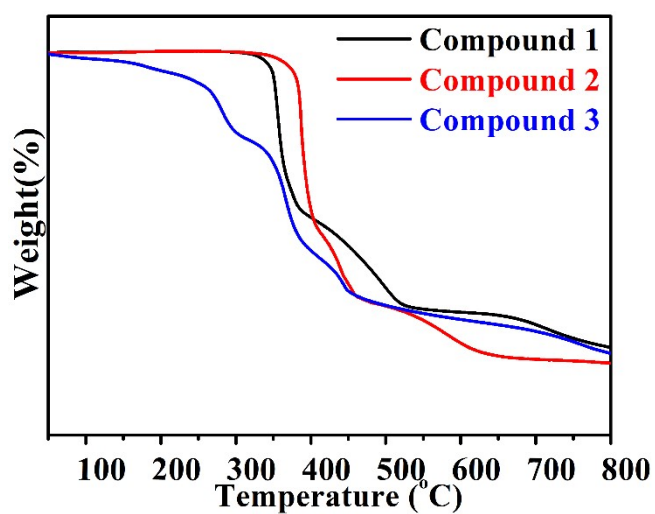


Figure S3. TGA curves for compound **1-3**.

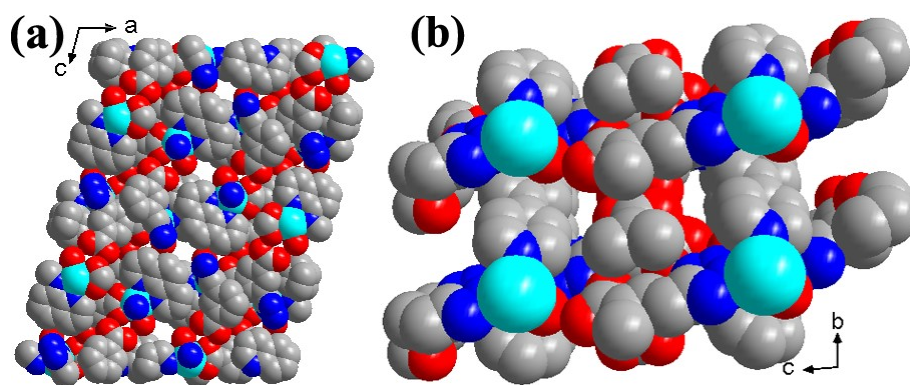


Figure S4. 3D supramolecular framework of compound 1 (a) and compound 2 (b).

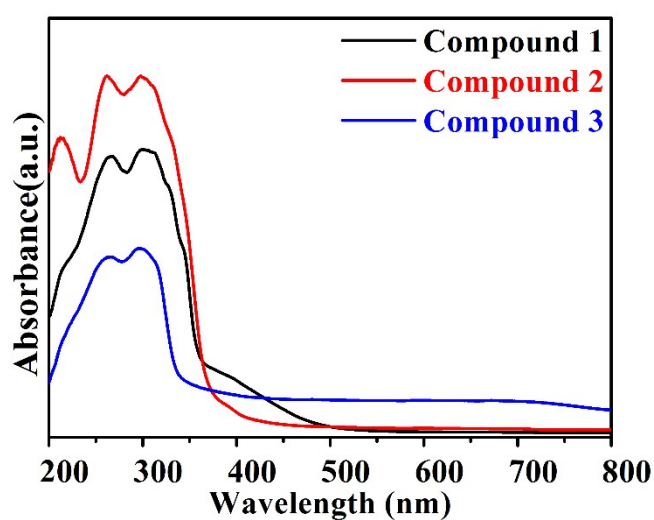


Figure S5. The solid-state UV-vis absorption spectra of compound 1–3 at room temperature.

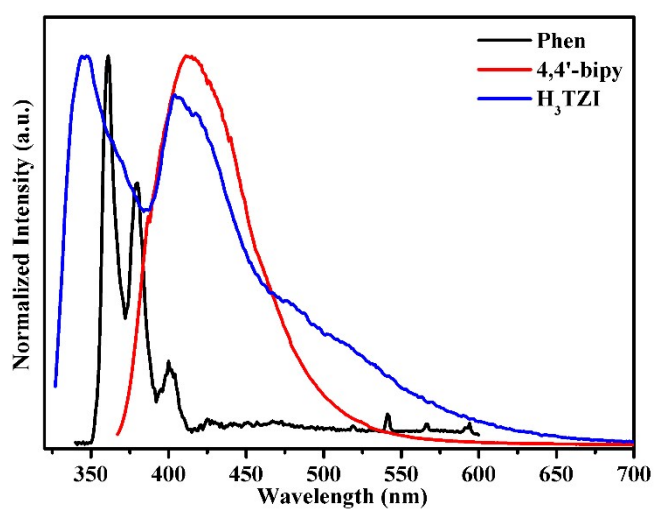


Figure S6. The photoluminescence spectra of ligands Phen, 4,4'-bipy and H₃TZI when excited at 320 nm.

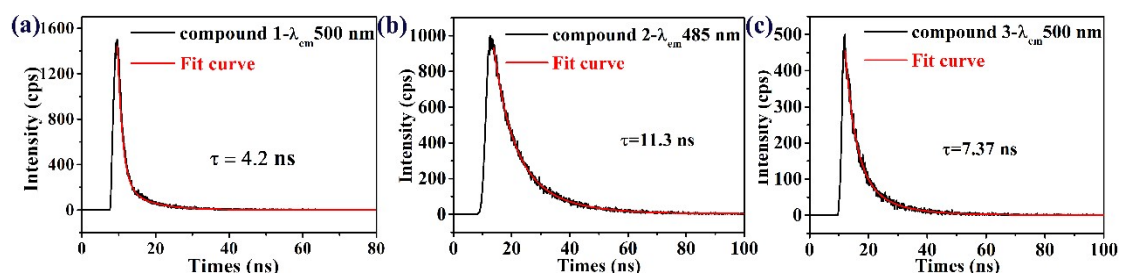


Figure S7. Fluorescence decay plot of compound 1-3.

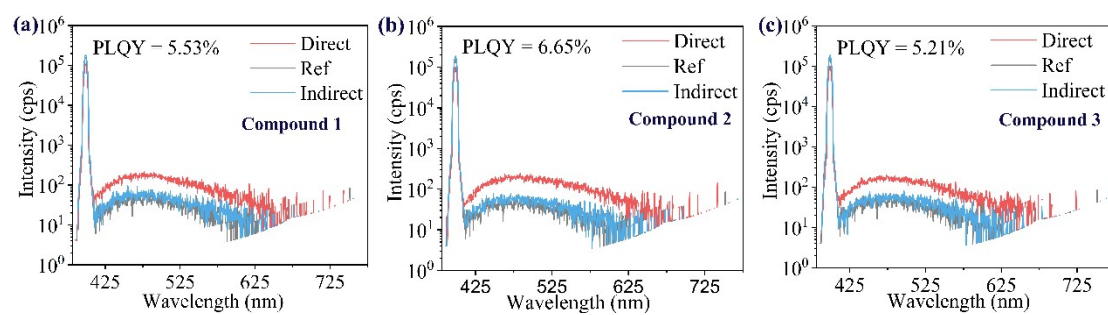


Figure S8. Quantum yield plot of compound 1-3 under 400 nm excitation and the emission wavelength is 500 nm, 485 nm and 500 nm, respectively.